Macromolecules

ARTICLE

pubs.acs.org/Macromolecules

# Fabrication of Lithographically Defined Chemically Patterned Polymer Brushes and Mats

Chi-Chun Liu,[†] Eungnak Han,[‡] M. Serdar Onses,[†] Christopher J. Thode,[†] Shengxiang Ji,[†] Padma Gopalan,[‡] and Paul F. Nealey*[,†]

[†]Department of Chemical and Biological Engineering and [‡]Department of Material Science and Engineering, University of Wisconsin—Madison, Madison, Wisconsin 53706, United States

Supporting Information

**ABSTRACT:** Chemically patterned surfaces comprised of polymer mats and brushes of well-defined chemistry were fabricated at the length scale of 10 nm. A key concept is the integration of new materials, cross-linked polymer mats, with traditional lithographic processing. Resist was patterned on top of cross-linked polystyrene mats. After etching, regions of the remaining mat with dimensions ranging from 10 to 35 nm were separated by interspatial openings to the underlying substrate. End-grafted polymer brushes, in this case hydroxyl-terminated poly(2-vinylpyridine) or polystyrene−poly(methyl methacrylate) random copolymer, were grafted into the exposed, interspatial regions from films spin-coated over the patterned mat. Both block copolymer wetting studies, with polystyrene-*block*-poly(methyl methacrylate) (PS-*b*-PMMA), and near-edge X-ray fine structure spectroscopy showed that with sufficient cross-linking the polymer mat chemistry was unaffected by the subsequent grafting of the polymer brush. The precise definition of both the chemistry and the geometry was demostrated with two sensitive applications of nanoscale chemical patterns: the site-specific immobilization of Au nanoparticles and the directed assembly of overlying PS-*b*-PMMA films.

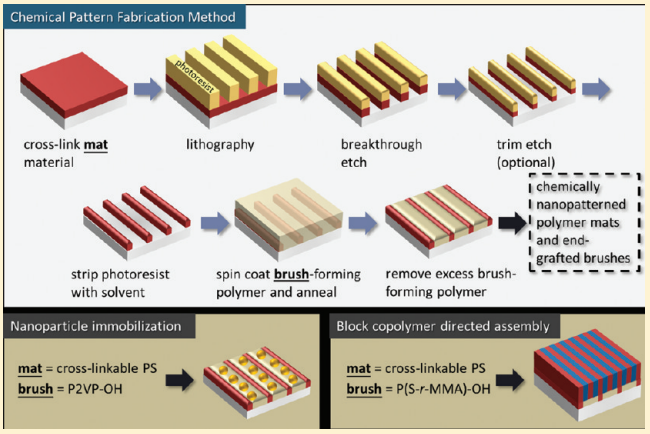


## I. INTRODUCTION

The fabrication of well-defined chemical patterns, in terms of both chemistry and geometry, is critical for a number of important applications.[1−5] Perhaps two of the most demanding applications are the directed assembly of block copolymers[6,7] and the site-specific immobilization of nanoparticles (NPs).[8,9] In the directed assembly of block copolymers, for example, patterns with at least one dimension of equivalent size to a single microphase-separated domain may be required. If these materials find use in manufacturing bit patterned media or semiconductor devices, scaling concerns imply that device features and chemical patterns will need to be created at dimensions below 10 nm.[10,11] In the case of NP immobilization, chemical patterning of the surface has proven to be a highly promising strategy for the specific placement of NPs as it provides robust and controllable substrate−particle interaction.[8,12] Many NPs or assemblies of NPs of technological interest, for example, plasmonic waveguide made of discrete NPs,[13] also have characteristic dimensions of tens of nanometers and require chemical patterns with equivalent dimensions.

Chemical nanopatterns have typically been fabricated in two different ways to achieve site-specific NP placement. In one general approach, self-assembled monolayers (SAMs) are deposited on lithographically defined regions of a silicon substrate, and then Au NPs are immobilized to the SAMs via electrostatic attraction. For example, lines of aminopropyltriethoxysilane (APTES) were deposited on silicon oxide after patterning poly(methyl methacrylate) (PMMA) photoresist with electron beam lithography, and negatively charged Au NPs subsequently adhered to the APTES.[14] In similar work, lithographically patterned lines of Au on silicon oxide could be used to fabricate patterns of SAMs, comprised of either APTES[15] on silicon oxide or amino-terminated alkanethiols on Au,[12] and then Au NPs were selectively immobilized on the amino groups. Although these techniques have been successful in immobilizing NPs, they have drawbacks. For example, the use of a lift-off process[14,15] imposes some limitations in that only a limited set of materials and conditions could be used for the functionalization and the lifting off of the particles and could lead to inconsistencies in the attachment of the remaining particles.

**Received:** December 16, 2010
**Revised:** February 16, 2011
**Published:** March 18, 2011

Chemical patterns designed for directed assembly of block copolymers often have been fabricated from a homogeneous thin organic film that was lithographically patterned and subsequently etched with an oxygen plasma to remove, either completely or partially, the film material in selected areas.[6,16−18] The initial film was formed from SAMs,[6] polymer brushes,[7,16,19,20] or polymer mats.[21] The etched regions of the film would be wet preferentially by one block of the copolymer, while the unetched regions would either be wet by the other block or be nonpreferential in wetting toward the two blocks. (Throughout this paper we will refer to the region with a strong preference to be wet by a specific block of the copolymer as the *guiding* region and the second region, which usually has an area greater than or equal to the guiding region, and could be either preferentially wet by the other block or nonpreferential to the two blocks, as the *background* region.) Because the guiding and background regions were derived from the same initial thin film, their chemistries could not be chosen independently. Moreover, the chemistry of the guiding regions was dependent on the etching conditions, and the chemistry of the protected regions could also be affected by the lithographic and etch processes.

The need for increasingly precise control of chemical pattern feature dimensions and chemistry has been highlighted by recent directed assembly results in which the assembled block copolymer feature density was an integral multiple of the chemical pattern feature density.[17,18,20,22,23] This increase in feature density, known as "density multiplication", yields an assembled pattern with greater resolution than the original, lithographically defined chemical pattern. Ruiz et al. and Detcheverry et al. used both experiments on and simulations of polystyrene-*block*-poly(methyl methacrylate) (PS-*b*-PMMA) directed to assemble with density multiplication on chemical patterns composed of hydroxyl-terminated polystyrene (PS-OH) brush, which had been patterned and subsequently oxidized. If the dimensions of the guiding regions of the block copolymer deviated significantly from the size of a block copolymer domain, or if the background chemistry were not optimum, defect-ridden assemblies or complex three-dimenisonal structures formed. Even in directed assembly without density multiplication, Edwards et al. demonstrated that the geometry and chemistry of the chemical pattern can affect the assembly dynamics,[24] the three-dimensional structure of the assembled domains,[25] and the uniformity and perfection of the equilibrated, assembled pattern.[16]

In this work, we demonstrate a chemical pattern fabrication method with precise control in chemistry and geometry utilizing specialized materials and lithographic patterning techniques. The principal idea involves two steps: (1) create a base imaging layer that retains its chemistry through processing but can be patterned by lithography and a sublithographic trim etch and (2) selectively deposit materials in the interspatial regions where the base imaging layer was removed after patterning. The process starts with the formation of a cross-linked polymer mat on the substrate, which is lithographically patterned and subsequently etched to expose the substrate in desired locations. Hydroxyl-terminated polymer brushes are then deposited and grafted to the exposed substrate to fill the interspatial regions. Importantly, throughout the entire process the chemistry of the polymer mat remains unchanged due to its high degree of cross-linking. Not only do the materials and process provide precise control of both the chemistry and the geometry of the chemical pattern, but they allow greater freedom in the choice of materials. We demonstrate the efficacy of chemical patterns formed in this manner by showing that the patterns can direct the assembly of block copolymers and also selectively immobilize Au nanoparticles in dense arrays.

## II. EXPERIMENTAL SECTION

**A. Materials.** Cross-linkable polystyrene (X-PS) containing 4 mol % of glycidyl methacrylate (GMA) was synthesized as described previously.[21,26] The X-PS used in this study, before cross-linking, had a number-average molecular weight ($M_n$, determined by gel permeation chromatography) of ∼60 kg/mol and a polydispersity index (PDI) of 1.4. PS-*b*-PMMA block copolymer (BCP), hydroxyl-terminated polystyrene (PS-OH), and hydroxyl-terminated poly(2-vinylpyridine) (P2VP-OH) were purchased from Polymer Source, Inc., and used as received. The PS-*b*-PMMA used in this study had a $M_n$, PDI, and bulk morphological period ($L_0$) of 37K-*b*-37K, 1.08, and ∼40 nm, respectively. The P2VP-OH had a $M_n$ of 6.2 kg/mol and a PDI of 1.05. The PS-OH had a $M_n$ of 6 kg/mol and a PDI of 1.07. Hydroxyl-terminated random copolymers of styrene and methyl methacrylate containing 43% and 60% of PS (P(S43-*r*-MMA)-OH and P(S60-*r*-MMA)-OH, respectively) were synthesized as before and had $M_n$ and PDI values in the range of 2−7.5 kg/mol and 1.2−1.4, respectively.[21] P(S60-*r*-MMA)-OH was used in the experiments of block copolymer directed assembly, and P(S43-*r*-MMA)-OH was used only in the near-edge X-ray absorption fine structure (NEXAFS) spectroscopy experiments. The PMMA used as the photoresist in the patterning process was purchased from MicroChem and had a molecular weight of 950 kg/mol. The photoresist was diluted from the original concentration (3 wt % in chlorobenzene) to 1.5 wt % using chlorobenzene. Toluene, *N*-methylpyrrolidone (NMP), GMA, dimethylformamide (DMF), and chlorobenzene were purchased from Aldrich and Fisher and used without further purification.

**B. Sample Preparation.** *Deposition of X-PS Mats.* A dilute solution of X-PS (0.25 wt % in tolune) was spin-coated at 4000 rpm onto a freshly cleaned silicon wafer, yielding a film 6−8 nm in thickness. The sample was heated to 160 C for 3 h or 190 C for 2 days under vacuum to drive the cross-linking reaction. The sample was then washed by repeated sonication in toluene to remove any residual uncross-linked X-PS.

*Patterning of X-PS Mats.* A 70 nm thick layer of photoresist was coated onto the cross-linked X-PS on the substrate. The photoresist was subsequently patterned with extreme ultraviolet interference lithography (EUV-IL)[27] to give a grating pattern consisting of parallel lines of width $W$ and period $L_s$ = 80 nm ($2L_0$), unless otherwise specified. $W$ ranged from 20 to 60 nm depending on the exposure dose. Some of the samples were etched with oxygen plasma[28] (10 mT, 10 sccm $O_2$, and 50 W in a Unaxis 790 RIE tool) to remove the X-PS in the regions exposed by lithography and in some instances to decrease $W$. The remaining photoresist was then removed with warm solvent (NMP or chlorobenzene) and repeated sonication.

*Deposition of Hydroxyl-Terminated Brushes.* Hydroxyl-terminated P(S-*r*-MMA)-OH was spin-coated from a 0.5 wt % toluene solution onto the samples, yielding a film ∼20 nm in thickness. The substrate was then annealed at 190 C for 4−72 h to graft the P(S-*r*-MMA)-OH onto the native oxide of the sample through a condensation reaction, resulting in a 5 nm thick layer of P(S-*r*-MMA). Excess P(S-*r*-MMA)-OH was washed away with toluene and sonication after the reaction. P2VP-OH was spin-coated from a 1.0 wt % DMF solution, annealed at 190 °C for 4 h, and then washed by sonication in DMF. The thickness of the P2VP brush was ∼4 nm. PS-OH was spin-coated from a 1.0 wt % toluene solution and annealed at 160 C for 1 h, followed by sonication in toluene to remove any excess material.

*Assembly of Block Copolymer Films.* On both chemically patterned and unpatterned substrates (for wetting behavior studies), PS-*b*-PMMA films were spin-coated from a 1.0−1.5 wt % solution in toluene and then

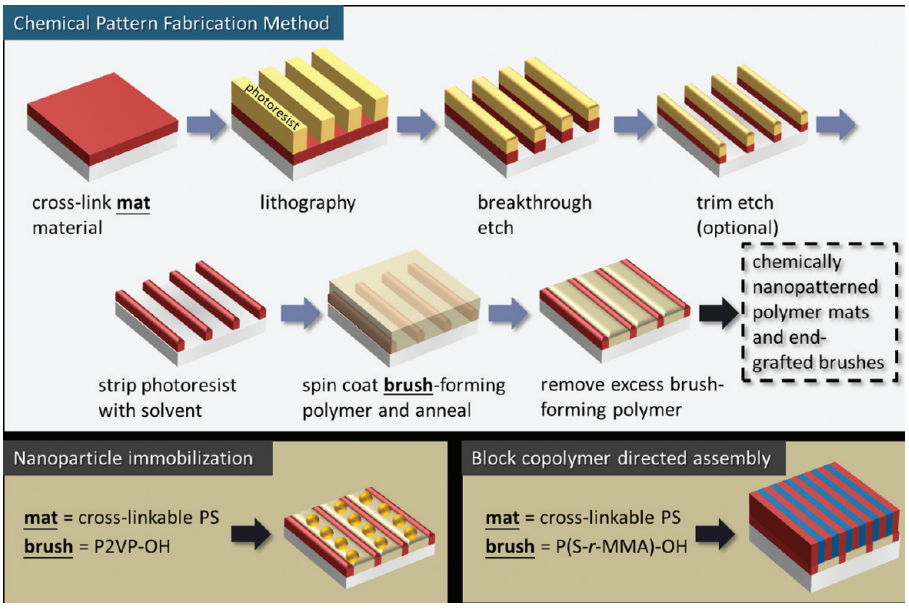


**Figure 1.** Schematic of the chemical pattern formation process, followed by nanoparticle immobilization or directed assembly. A film of cross-linkable polystyrene (X-PS) is cross-linked, patterned, and etched. Subsequently, P(S-*r*-MMA)-OH is grafted onto the exposed spaces of the substrate to complete the chemical pattern. Different brush materials could be chosen according to the need. For example, a film of PS-*b*-PMMA is directed to assemble on the chemical pattern with P(S-*r*-MMA)-OH brushes, and nanoparticles could be immobilized by using P2VP-OH brushes.

annealed for 1 h at 250 C in a nitrogen environment. When desired, the PMMA domains were removed with $O_2$ plasma, using the same condition as in patterning the X-PS mats.

*Synthesis and Immobilization of Gold Nanoparticles.* Gold nanoparticles (Au-NPs) were synthesized using a citrate reduction of $HAuCl_4$ in water, following previously published methods.[29] Au-NPs were diluted to a concentration of ~2 nM for the immobilization experiments. Substrates with chemical patterns were immersed in the Au-NP solution for 30 min, washed in water under ultrasonic agitation for 2 min, and then blown dry with $N_2$.

**C. Analysis.** *Characterization of Wetting Behavior of BCP Films on Surfaces.* The wetting behavior on chemically homogeneous substrates before and after exposure to the P(S-*r*-MMA) grafting procedure was determined by analyzing the topography (island or hole) of an assembled BCP film whose thickness was incommensurate with an integral multiple of $L_0$.[30−32] This "island/hole" experiment[32] was performed on three types of substrates: bare Si (with native oxide), 6 nm X-PS cross-linked at 160 °C for 3 h, and 6 nm X-PS cross-linked at 190 °C for 2 days. Two pieces of each type of substrate were prepared, and one of them was processed with the P(S-*r*-MMA) grafting procedure as described earlier. A ~30 nm thick film of PS-*b*-PMMA was then assembled on these substrates, and the topography was observed with a scanning electron microscope (SEM).

*Near-Edge X-ray Absorption Fine Structure (NEXAFS) Spectroscopy.* NEXAFS experiments and analyses were performed at the Synchrotron Radiation Center of the University of Wisconsin—Madison, using the 10 m TGM beamline as described previously, and focusing on the C 1s spectra.[33,34] Substrates with X-PS cross-linked at 190 °C for 2 days were spin-coated with a layer of P(S43-*r*-MMA)-OH and then annealed at 190 °C for times ranging from 4 to 72 h, followed by rinsing with toluene to remove any ungrafted material. Results were compared to two control samples: (1) a substrate with an X-PS mat that was not subject to the process of grafting the random brush and (2) a Si substrate on which P(S43-*r*-MMA)-OH brush was grafted for 4 h at 190 °C.

*Scanning Electron Microscopy (SEM) and Atomic Force Microscopy (AFM).* A LEO 1550VP field-emission SEM and a Veeco MultiMode scanning probe microscope with tapping mode were used to image the chemical patterns, assembled block copolymer films, and samples with adsorbed Au-NPs.

## III. RESULTS

A schematic illustration of the process used to create the chemical patterns in this study is shown in Figure 1. The method started with the deposition of an X-PS mat on a Si substrate, followed by lithographic patterning of a photoresist on top of the mat. The pattern on the photoresist was then transferred to the X-PS via an oxygen plasma etch (the "breakthrough etch"). The etch time for the breakthrough step was determined by the thickness of the X-PS, which could be controlled via the spin-coating process, and the etch rate under the given processing parameters. If the width of the photoresist and subsequently the X-PS lines were wider than desired, i.e., in circumstances in which sublithographic patterning is required, an additional etching step was implemented following the breakthrough etch. This additional etching step employed a controllable lateral etch rate for fine dimension control and is referred to as the "trim etch". In this work, we simply used an extended etching time with the same reactor conditions, longer than required by the breakthrough etch, for the trim etch. After the etching of the X-PS in the exposed areas, the photoresist protecting the remaining patterns of X-PS was removed by solvents. The interspatial regions could then be functionalized with polymer brushes of different chemistry, for example, P(S-*r*-MMA)-OH or P2VP-OH, through a condensation reaction of the reactive −OH end groups with the substrate.

Two important features of the fabrication process for chemical pattern formation are apparent: first, the pattern geometry, including the line width and height and the thickness variation of the polymer mat, can be precisely controlled, and second, the chemistry of the polymer mat structures and the interspatial regions of the chemical patterns can be controlled independently. The chemically patterned substrates can then be used to

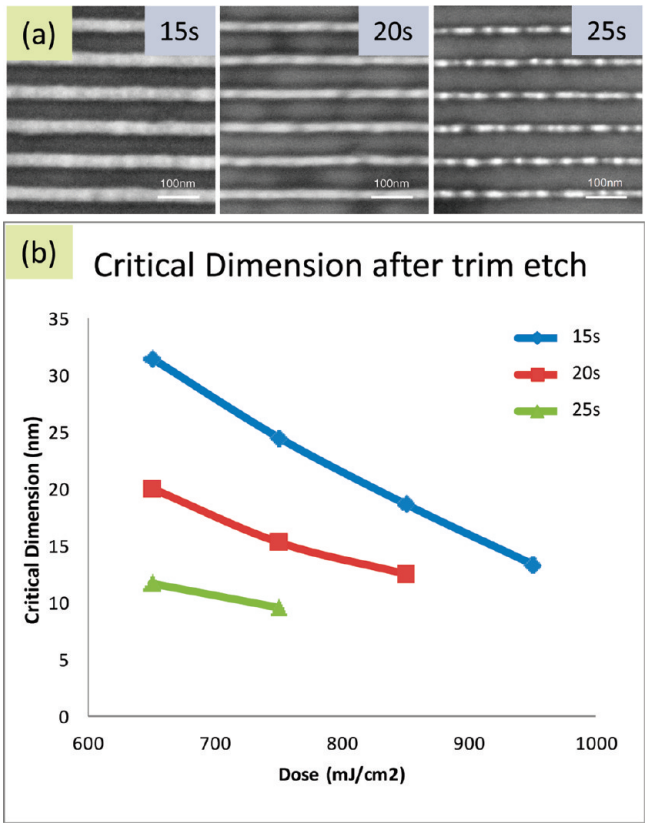


**Figure 2.** (a) Top-down SEM images from samples with the same exposure doses during lithography but different $O_2$ etch times. (b) Effect of exposure dose and trim etch time (shown in the legend) on the critical dimension (CD) of the pattern.

direct the assembly of PS-*b*-PMMA films, or to immobilize Au-NPs, into the desired patterns. In the directed assembly case, the X-PS lines of the chemical pattern were the guiding patterns, and the area covered by the random copolymer was the background region. The desired chemical pattern for directed assembly of a symmetric BCP should be composed of guiding patterns with width $W \sim 0.5L_0$, and with a strong wetting preference to one of the blocks in the BCP, while the wetting preference of the background region should be adjustable according to the specific BCP system.[35] For Au-NP immobilization, the guiding patterns should have minimal adsorption of the NPs while the background should have a strong adsorption, or vice versa.

The line width of the chemical pattern may be controlled by changing the dimensions of the photoresist patterns and the trim etch. Figure 2a shows the results of a constant exposure dose with various etch times, which were the sum of both the breakthrough etch and the trim etch, to tune the line width from ~1/2 of the pitch to almost 1/8 of the pitch. As shown in Figure 2b, the line width could be varied from 15 to ~35 nm by changing the exposure dose in the lithography process for a given etch time.

The relative height between the guiding lines and the background can be controlled by the initial thickness of the X-PS. The thickness of the P(S-*r*-MMA) used in this work was ~5 nm, which was controlled by the $M_n$ of the random copolymer and the time of grafting reaction.[36,37] Starting with a 7 nm thick film of X-PS, the final structure after the random brush deposition had a ~2 nm topography change. Figure 3a,b shows the SEM images of the X-PS stripes before and after the grafting of the P(S-*r*-MMA)-OH, respectively. The contrast was higher in Figure 3a than its counterpart after the brush deposition because both the material contrast (polymer vs Si) and the topographic contrast (~7 nm) were greater before the deposition. After the deposition (Figure 3b), there was almost no contrast in material (X-PS vs P(S-*r*-MMA)-OH), and the topography difference, as measured by AFM (Figure 3c–f), was much lower. An increase in the height variation of the X-PS after the brush grafting was observed, but on the basis of additional experiments, we believe that the variation was not caused by the grafting process (see Supporting Information). It should be noted that if a larger topography change were desired, it is straightforward to achieve such a condition by starting with a thicker X-PS.

Although one may choose different cross-linkable materials and hydroxyl-terminated random copolymers to create chemical patterns with a range of functionalities, one of the major challenges for controlling the chemistry precisely is to prevent the chemistry of the cross-linkable guiding stripes from being modified during the deposition of the brush in the interspatial region. In particular, it is possible that the hydroxyl-terminated brushes may (1) react with the X-PS (e.g., at unreacted cross-linking sites), (2) diffuse through the X-PS mat and react with the surface covered by the X-PS, or (3) be entrained in the X-PS mats. For example, during the deposition of the P(S-*r*-MMA)-OH brush in the X-PS/P(S-*r*-MMA)-OH system, both the X-PS stripes and the non-X-PS-covered region will be exposed to the P(S-*r*-MMA)-OH, the deposition conditions, and the solvent treatment, as shown in Figure 1, step 6. We hypothesized that if the cross-linking density of the mats is sufficiently high and the cross-linking reaction is virtually complete, such that there are very few remaining functional groups in the X-PS, all three undesirable mechanisms listed above could be suppressed. To test our hypothesis, X-PS films were baked at 160 °C for 3 h or at 190 °C for 48 h to drive the cross-linking reaction. The mats cross-linked under the latter condition should have a higher cross-linking density and fewer unreacted GMA groups and therefore should be less susceptible to chemical modification by the P(S-*r*-MMA)-OH.

In an experiment to study the effect of the P(S-*r*-MMA)-OH deposition process on the chemistry of the X-PS as a function of the X-PS deposition condition, the change in wetting behavior of PS-*b*-PMMA thin films was investigated. If a homogeneous layer of X-PS were modified by P(S60-*r*-MMA)-OH brush deposition, the surface of the X-PS would change from preferential to PS wetting to weakly preferential or nonpreferential to PS wetting. In the "island/hole" experiment described in the Experimental Section, the surface chemistry of the cross-linked X-PS mat affects the wetting behavior of the PS-*b*-PMMA and also its morphology after block copolymer phase separation. Therefore, an "island/hole" experiment can be used as a sensitive indicator of the substrate chemistry.[31,38,39] The morphology after phase separation, using the given copolymer film thickness, can be either an "island" structure (Figure 4a, the continuous phase is lower than the discrete phase and hence shows darker contrast under SEM), a "hole" structure (Figure 4c, the continuous phase is raised and higher than the discrete phase), or a flat surface (Figure 4b, the feature under higher magnification showed a fingerprint-like morphology) when the surface of the substrate is PMMA-preferential, PS-preferential, or nonpreferential, respectively. The initial thickness of the block copolymer allows the interpretation of the results in this method. The first column in Figure 4 shows the morphologies on different types of substrates

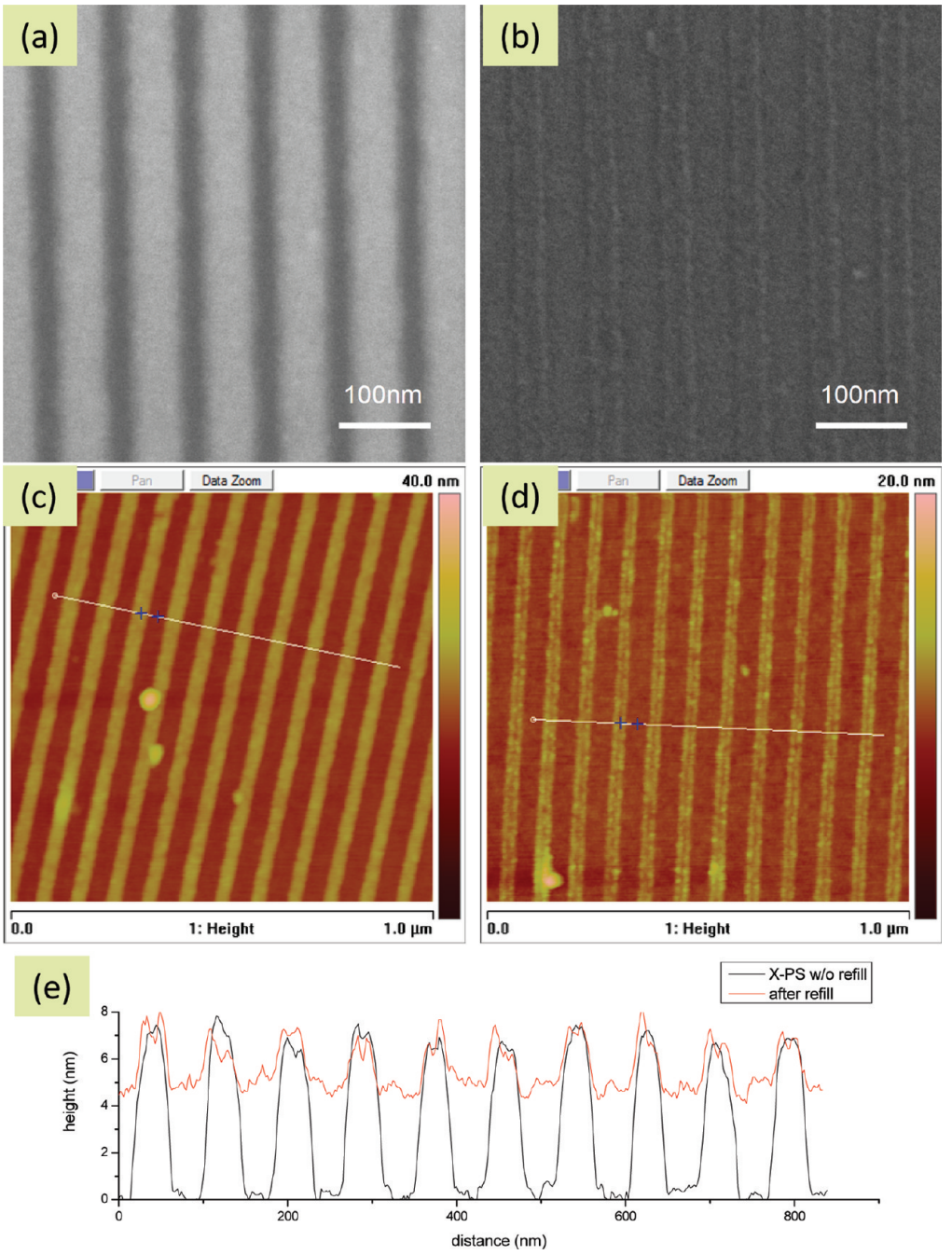


**Figure 3.** SEM and AFM analysis of chemical pattern fabrication process. Top-down SEM images of cross-linkable polystyrene (X-PS) (a) before and (b) after grafting P(S-*r*-MMA)-OH. AFM images of X-PS (c) before and (d) after grafting. (e) Cross-sectional profile along the lines shown in (c) and (d) in black and red, respectively.

that have not undergone the random-OH deposition process. The native oxide surface of a silicon substrate was PMMA-preferential and thus exhibited an "island" structure for this film thickness (Figure 4a). The surface of the BCP film on the X-PS substrates (Figure 4c,e) exhibited a "hole" structure, indicative of a PS-preferential surface, regardless of X-PS cross-linking conditions. In contrast, substrates that underwent the random-OH deposition process exhibited markedly different wetting behaviors, as shown in the second column of Figure 4. The grafted Si surface was nonpreferential (Figure 4b), as one would expect based on previous work with P(S-*r*-MMA) brushes containing 60% S.[16,36,40,41] A similar fingerprint structure was also observed in the PS-*b*-PMMA film on the surface consisting of X-PS cross-linked at 160 °C for 3 h followed by P(S-*r*-MMA)-OH grafting (Figure 4d), showing that this surface was also nonpreferential. The nonpreferential nature of the surface implied that this cross-linking condition was not sufficient to prevent the X-PS from being modified by the random brushes. On the other hand, the X-PS cross-linked at 190 °C for 2 days remained PS-preferential after the grafting process.

Although the "island/hole" test is sufficient for determining suitable cross-linking conditions for which the X-PS remains

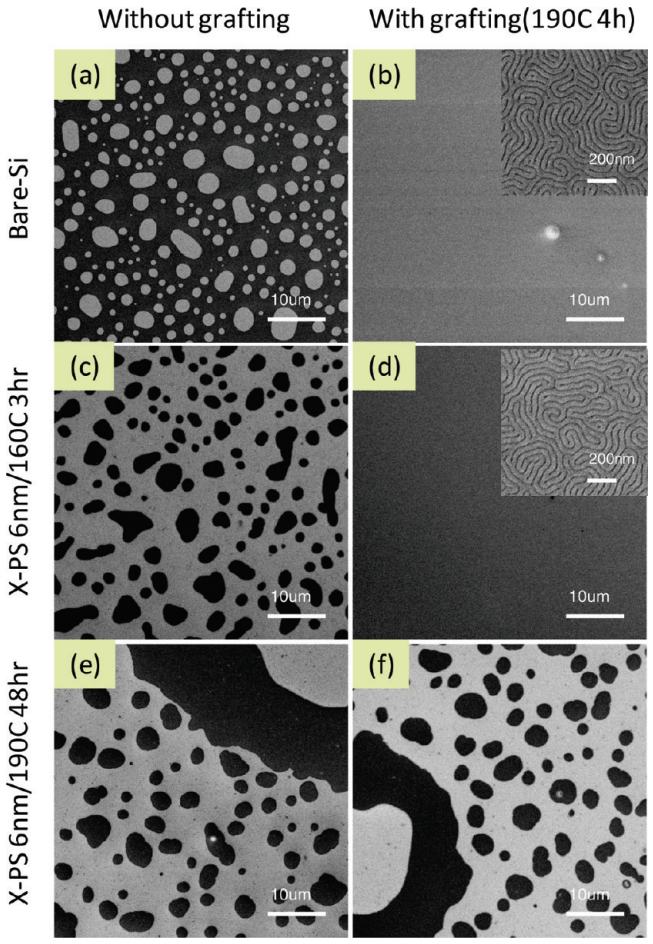


**Figure 4.** SEM images of the surface of a PS-*b*-PMMA film on top of an array of different substrates. Three different substrates were used, as shown on the left. The X-PS grafting conditions are shown for the second and third rows. The substrates in the left column were not exposed to the grafting of nonpreferential P(S-*r*-MMA)-OH at 190 C for 4 h, whereas the substrates in the right column were. On the basis of the island−hole or fingerprint structures that formed in the PS-*b*-PMMA film, the substrates can be experiment results can be interpreted as (a) PMMA-preferential, (b) nonpreferential, (c) PS-preferential, (d) nonpreferential, (e) PS-preferential, and (f) PS-preferential.

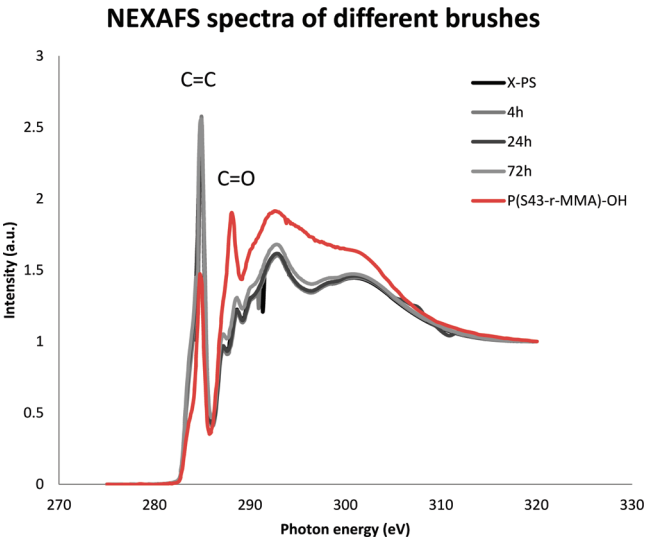


**Figure 5.** C 1s near-edge X-ray absorption fine structure (NEXAFS) spectra of cross-linked X-PS initially and after exposure to P(S43-*r*-MMA)-OH (43% PS) brush grafting for various times. For reference, the NEXAFS spectra of P(S43-*r*-MMA)-OH grafted to a clean silicon wafer (190 °C for 4 h) is also shown. The location of the peaks corresponding to the C═C and C═O 1s to $\pi^*$ transitions (285.2 and 288.5 eV, respectively) are indicated on the graph. The X-PS mat was not affected by the brush grafting process, as evidenced by the overlap of the spectra and the lack of a C═O peak.

PS-preferential in wetting behavior, it does not preclude the possibility of some chemical modifications. Previous studies showed that P(S-*r*-MMA)-OH brushes with 80−100% PS content exhibit similar PS-preferential wetting behavior in such a test. Because there could be some minor modifications of the X-PS that cannot be discerned with the "island/hole" test, near-edge X-ray absorption fine structure (NEXAFS) spectroscopy was used to provide another, very sensitive method of viewing the extent of chemical modifications that might occur. Previous research has shown that a linear combination of the spectra of the two polymers in a random copolymer can be used to determine the composition of the copolymer.[34] For the materials in this study, the most noteworthy features of the C 1s spectra of PS and PMMA are the C═C 1s to $\pi^*$ transition (285.2 eV) of the aromatic group in PS and the C═O 1s to $\pi^*$ transition (288.5 eV) of the carbonyl group in PMMA.[42] Figure 5 shows the NEXAFS spectra for a X-PS mat that had been cross-linked at 190 C for 2 days as well as the spectra for P(S43-*r*-MMA)-OH grafted on silicon, for the sake of comparison. The X-PS mat was subjected to P(S43-*r*-MMA)-OH brush deposition at 190 °C for durations ranging from 4 to 72 h. None of the samples in which the X-PS mat was exposed to the P(S43-*r*-MMA)-OH grafting process contained the C═O peak. Instead, the spectra of the X-PS substrates did not change after undergoing a random brush deposition process from 4 to 72 h and overlapped with the ungrafted X-PS very well, indicating that there was minimal (<5%),[34] if any, PMMA present in the X-PS after the grafting process.

The importance of both the chemistry and the geometry of the chemical pattern can be demonstrated by BCP assembly with density multiplication ($L_s = 2L_0$), as shown in Figure 6. Directed assembly with density multiplication has been predicted to be very sensitive to both chemistry and geometry[23] and hence provides a stringent test for the X-PS/P(S-*r*-MMA)-OH system. A chemical pattern with a suitable line width of X-PS ($W/L_0 \sim 0.5-0.7$), but without any brush deposited in the background region, was not able to direct the assembly of uniform perpendicular structures of PS-*b*-PMMA. Instead, a mixture of parallel and perpendicular structures was formed, as shown in Figure 6a. In contrast, if the line width of the X-PS was significantly larger than $L_0/2$ but the background region had the proper brush deposited, as demonstrated in Figure 6b with $W/L_0 \sim 0.8$, the PS-*b*-PMMA formed mostly perpendicular structures, but with a number of defects. Only when the chemistry and the geometry of the chemical pattern were both properly defined with $W/L_0 \sim 0.5$ and P(S-*r*-MMA) grafted in the interspatial regions could a perfect directed assembly of PS-*b*-PMMA be obtained, as shown in Figure 6c. For the thickness of the PS-*b*-PMMA films and the imaging conditions used in this study, the guiding patterns could be seen through the PS-*b*-PMMA film, and as a result, there are two different contrasts of the assembled PS lines in Figure 6a−c.

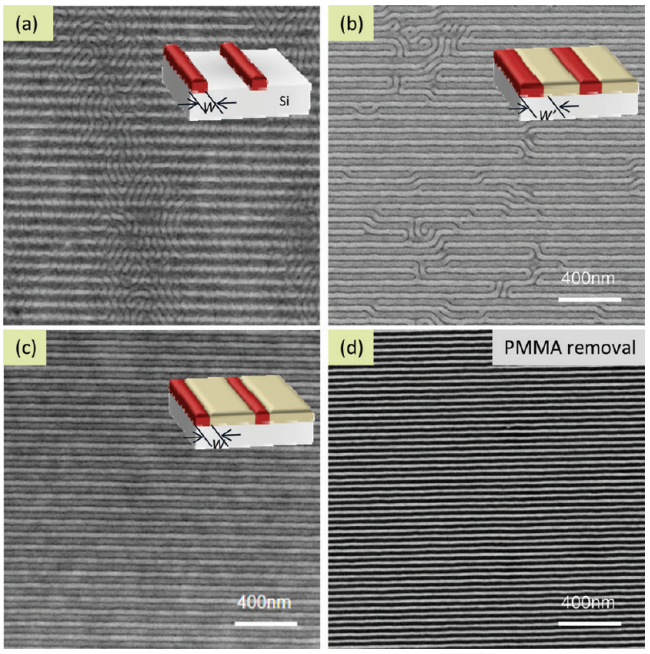


**Figure 6.** Importance of using the correct line width and background chemistry on the directed assembly of PS-*b*-PMMA on a chemical pattern with $L_s = 2L_0$. The chemical patterns were composed of (a) correct line width ($W \sim 20$ nm $= L_0/2$) but incorrect background chemistry (bare silicon) in the background, (b) incorrect line width ($W' \sim 32$ nm) but correct chemistry (nonpreferential P(S-*r*-MMA) brush) in the background, and (c, d) correct line width and background chemistry, with the PMMA block removed in (d). The insets illustrate the chemical patterns used in each case. The red stripes represent the X-PS guiding patterns, and the yellow stripes represent P(S-*r*-MMA) background.

After selectively removing the PMMA blocks with $O_2$ plasma,[43,44] the PS structures can be seen more clearly as in Figure 6d.

Another application of chemical patterns is the controlled placement and immobilization of nanoparticles.[8,9] P2VP is known to have good binding strength with many nanoparticles via the formation of a covalent bond between pyridine and the metal through the donation of the lone pair of electrons of the nitrogen atom,[45] while PS can be used as a protective material to prevent nonspecific adhesion on the substrate. Because each repeating unit on a P2VP polymer chain can be a binding site for metal nanoparticles, it only requires a few P2VP chains on a PS surface to immobilize an Au-NP. Because of the affinity of P2VP repeat units for Au-NPs, this Au-NP immobilization experiment can also be used as a sensitive test for the detection of surface modification, similar to the island/hole test used above. Similar to the NEXAFS experiment, P2VP-OH was deposited (at 190 °C for 4 h) on three types of nonpatterned substrate: (1) a bare Si wafer with native oxide, (2) X-PS cross-linked at 160 °C for 3 h, and (3) X-PS cross-linked at 190 °C for 48 h. The substrates were then used for an immobilization test with Au-NPs and then inspected by SEM (Figure 7a−c). The particle surface density data shown in Figure 7a−c were obtained by inspecting several SEM images and averaging over a ~80 $\mu m^2$ area for Figure 7b and ~680 $\mu m^2$ for Figure 7c. The X-PS cross-linked at 190 °C for 48 h had the lowest Au-NP density, which suggests that it is the least likely to be chemically altered by the treatment with the hydroxyl-terminated brushes.

Following on the Au-NP immobilization tests with homogeneous substrates, the immobilization of Au-NPs on chemical patterns fabricated with a PS-OH/P2VP-OH system (Figure 7d) and a X-PS/P2VP-OH system (Figure 7e) was tested. As shown in Figure 7d, many Au-NPs adsorbed onto the regions coated with the PS-OH brush, suggesting that it was insufficient to prevent the penetration of P2VP-OH during the P2VP-OH deposition. In contrast, when cross-linked X-PS was used in place of PS-OH, specific adhesion and immobilization were achieved, with Au-NPs covering the P2VP interspatial regions, but not the X-PS lines (pattern $L_s = 110$ nm, Figure 7e). The lack of Au-NPs on the X-PS region showed that the grafting of the P2VP-OH to the substrate had little effect on the cross-linked X-PS.

## IV. DISCUSSION

The materials and processes presented here to fabricate chemically patterned surfaces at the nanoscale are compatible with ultrahigh resolution (e.g., electron beam) and massively parallel (e.g., EUV, 193 nm) lithographic techniques. The starting point for creation of the chemical patterns relates to the highest quality resist structures that may be achieved using the infrastructure of the semiconductor industry in terms of feature size, uniformity, and patterned area (300 mm wafers). Compatibility with generic photolithography processes is an important consideration for the integration of chemical patterns into semiconductor fabrication processes. Otherwise, a wafer-scale chemical pattern would be more difficult to achieve economically. As shown in Figure 1, the patterned lines in the proposed method were made with lithography and an $O_2$ plasma etch. Although EUV-IL was used to pattern the PMMA resist in this work, the patterning step in this process is inherently compatible with 193 nm lithographic processes because PMMA is also sensitive to 193 nm irradiation.[46] Indeed, the PMMA resist is merely a patterning intermediate in our method, and therefore a variety of exposure tools and lithographic processes could be used with our proposed process. Of course, processing issues specific to 193 nm lithography, such as the need for an antireflective coating (ARC) layer for subwavelength features, would need to be addressed before our method presented here could be implemented.[47]

A trim etch is often used after the lithography process because it provides an important process latitude for CD control, especially when the feature size is sublithographic. The pitch of the pattern is determined by the design of the mask used in photolithography, but the line width can be tuned by exposure dose and/or trim etch as demonstrated earlier. However, for the chemical pattern fabrication processes in which the mat and brush materials are derived from the same source, or deposited prior to the trim etch, to perform a trim etch on the mat and simultaneously control the chemistry of the brush, the brush region would need to be either protected during the trim etch or replaced afterward. Thus, we designed our fabrication method to graft the brush in the background region after the guiding stripes were formed. Furthermore, the width of the background region is complementary to the guiding stripes and therefore is also determined by the trimming of the guiding lines.

In terms of pattern chemistry, the control of the chemistry is achieved by forming a highly cross-linked mat that can undergo patterning and brush deposition processes without significantly affecting its surface chemistry. The work above demonstrates that the brush could be P2VP-OH or P(S-*r*-MMA)-OH, but one may choose different cross-linkable materials and hydroxyl-terminated

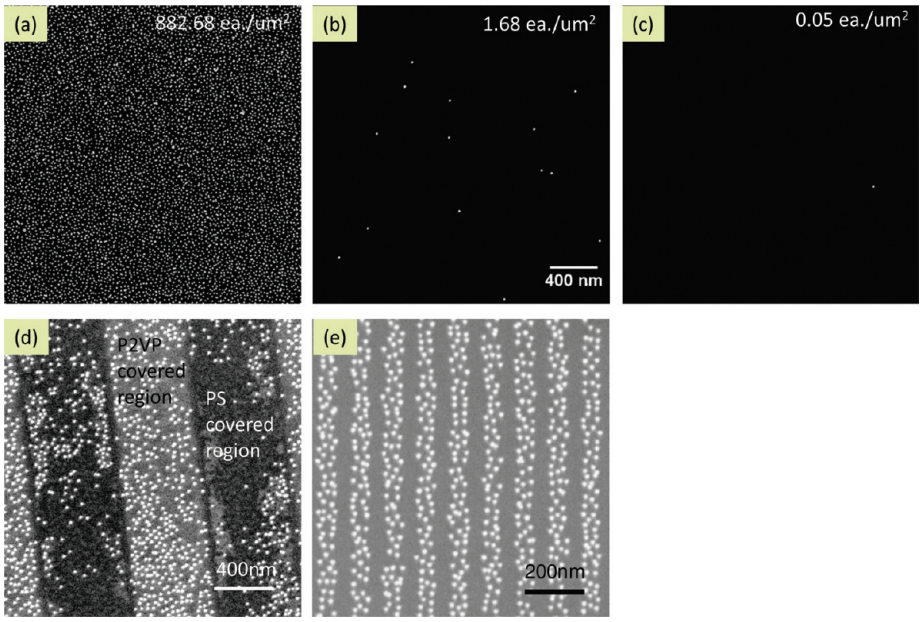


**Figure 7.** SEM images of gold nanoparticles adsorbed on homogeneous substrates (a−c, both are 2.5 × 2.5 $\mu m^2$) and chemical patterns (d, e.) The homogeneous substrates are prepared by grafting P2VP-OH at 190 °C for 4 h on (a) bare Si substrate, (b) X-PS cross-linked at 160 °C for 3 h, and (c) X-PS cross-linked at 190 °C for 48 h. The chemical patterns are composed of (d) PS-OH/P2VP-OH and (e) X-PS/P2VP-OH. (d) has patterns with large feature size while (e) has line patterns with period of 110 nm. The X-PS/P2VP-OH system shows much better specific adsorption behavior.

random copolymers to create chemical patterns with a range of functionalities. The chemical pattern fabrication method presented in this work differs from previous work on the selective immobilization of NPs at the nanoscale in important ways. For example, in our chemical pattern fabrication method, no material removal is needed after NP deposition, unlike those processes that used photoresist and APTES to force selective NP immobilization had a subsequent photoresist lift-off step.[12,14] Additionally, some former NP deposition processes required the formation of Au lines for the attachment of SAMs and the subsequent immobilization of NPs.[15] In our case, no additional metal is needed for the NP deposition beyond that of the NP itself.

In previous approaches for directed assembly of block copolymers,[6,16−18] the chemistry of the guiding patterns and the background could not be chosen independently. No matter whether the film material served as the guiding pattern and the etched material as the background or vice versa, the film material and the etched material were always coupled together and not selected independently. Other methods have used materials that could be selected independently, but only to a limited extent due to their requirement to perform as a photoresist or an ARC layer. For example, one approach used 193 nm lithography combined with lift-off patterning to create background regions of nonpreferential material and guiding lines of exposed antireflective coating material.[48] While this method was compatible with 193 nm lithography, and could make use of a trim etch to tune line widths, the chemistry choices for the guiding lines are limited to the ARC layer. An alternative method deposited a homogeneous brush layer first and then utilized a patterned negative photoresist over the brush layer as a guiding stripe.[22] The use of a negative photoresist as a guiding stripe served to decouple the background chemistry from the guiding stripes, but the method lacked the ability to tune precisely the line width with a trim etch, nor could the chemistry be controlled or assured.

The effectiveness of a chemical pattern depends in large part on the surface chemistry of the materials that compose the patterned features and the interspatial regions. The chemistry of the interspatial regions, which in our case is determined by the composition of the random copolymer brushes, can be controlled by polymer synthesis. However, side effects of the processing steps, such as photoresist residue, base developer, and photon damage, may add an uncertainty in the final effective surface chemistry of the brush. The molecular simulations in the work of Ruiz et al. and Detcheverry et al.[17,23,35] suggested that the polymer−substrate interfacial energy, which correlates to the brush composition, could affect the profile of the structures in the case of density multiplication. In this work, the background region was formed as the last step in the process so that the random brushes would not be in contact with any of the possible materials that can alter its chemistry. One can expect the least shift in the apparent brush composition with this approach. Because our method can eliminate interferences from the fabrication process and independently control the chemistry of the patterned features and interspatial regions, it provides a great opportunity to explore directed assembly further.

Besides forming an X-PS mat on top of the substrate, a sufficient bonding between X-PS stripes and the substrate is also important for chemical pattern fabrication. We believe the X-PS brushes used in this work can be considered similar to side-chain grafting hydroxyethyl methacrylate (HEMA) brushes, which were shown to be similar to hydroxyl-terminated brushes in their ability to direct the assembly of a block copolymer film.[21,49] The key difference between the X-PS brushes used in this study and the HEMA brushes is that each GMA group in the X-PS brushes used here will generate two hydroxyl groups during the cross-linking reaction. Therefore, for GMA and HEMA brushes with equivalent $M_n$ and mole fraction of the cross-linkable group, when reacted to completion the GMA system will have twice the cross-linking density and the grafting density as the HEMA

system. As a result, we would expect not only the X-PS to be cross-linked but also the adhesion of the GMA brush system to the native oxide on a silicon wafer to be at least equal to that of a HEMA brush system and therefore sufficient to anchor a chemical pattern to the substrate.

## V. CONCLUSION

In this paper, a fabrication method that allows precise, independent control of both the geometry and the chemistry of the chemically patterned substrates was presented. The process is based on the patterning of a highly cross-linked polymer mat. While this study focused on the use of a cross-linked PS mat, the method should apply to any polymer mat that can achieve a cross-link density that is high enough to prevent it from being altered by subsequent processing. The high cross-link density allows subsequent processing, such as trim etching and grafting of polymer brushes in interspatial regions, without having a deleterious effect on the chemistry of the patterned cross-linked mat. Examples of directed assembly of block copolymer and selective nanoparticle immobilization demonstrated the quality of the chemical pattern. The ability to improve the control of both the geometry and the chemistry of chemical patterns should provide a great opportunity for both scientific studies of processes relying on surface chemistry as well as technological applications of chemical patterns.

## ■ ASSOCIATED CONTENT

**Supporting Information.** Figure S1. This material is available free of charge via the Internet at http://pubs.acs.org.

## ■ ACKNOWLEDGMENT

C.C.L. thanks Artak Isoyan and John Wallace for the help with extreme ultraviolet lithography exposures and Gordon S. W. Craig for manuscript preparation and critical suggestions. He also thanks Yuk-Hong Ting for the discussions in etching process and Jingjing Liu for taking the AFM images. A portion of this work was supported by the Laboratory Directed Research and Development program at Sandia National Laboratories. Sandia is a multiprogram laboratory operated by Sandia Corporation, a Lockheed Martin Company, for the United States Department of Energy's National Nuclear Security Administration under Contract DE-AC04-94AL85000. This work was also supported by the Semiconductor Research Corporation, through project 2008-DJ-1884, and the National Science Foundation NSF through the Nanoscale Science and Engineering Center DMR-0832760. This work was based in part upon researches conducted at the Synchrotron Radiation Center, University of Wisconsin—Madison, which is supported by the NSF under Award DMR-0537588.

## ■ REFERENCES

(1) Xia, Y. N.; Whitesides, G. M. *Annu. Rev. Mater. Sci.* **1998**, *28*, 153–184.
(2) Rogers, J. A.; Bao, Z.; Baldwin, K.; Dodabalapur, A.; Crone, B.; Raju, V. R.; Kuck, V.; Katz, H.; Amundson, K.; Ewing, J.; Drzaic, P. *Proc. Natl. Acad. Sci. U.S.A.* **2001**, *98* (9), 4835–4840.
(3) Shah, R. R.; Merreceyes, D.; Husemann, M.; Rees, I.; Abbott, N. L.; Hawker, C. J.; Hedrick, J. L. *Macromolecules* **2000**, *33* (2), 597–605.
(4) Lee, K. B.; Park, S. J.; Mirkin, C. A.; Smith, J. C.; Mrksich, M. *Science* **2002**, *295* (5560), 1702–1705.
(5) Healy, K. E.; Thomas, C. H.; Rezania, A.; Kim, J. E.; McKeown, P. J.; Lom, B.; Hockberger, P. E. *Biomaterials* **1996**, *17* (2), 195–208.
(6) Kim, S. O.; Solak, H. H.; Stoykovich, M. P.; Ferrier, N. J.; de Pablo, J. J.; Nealey, P. F. *Nature* **2003**, *424* (6947), 411–414.
(7) Stoykovich, M. P.; Muller, M.; Kim, S. O.; Solak, H. H.; Edwards, E. W.; de Pablo, J. J.; Nealey, P. F. *Science* **2005**, *308* (5727), 1442–1446.
(8) Chai, J.; Wang, D.; Fan, X. N.; Buriak, J. M. *Nature Nanotechnol.* **2007**, *2* (8), 500–506.
(9) Glass, R.; Moller, M.; Spatz, J. P. *Nanotechnology* **2003**, *14* (10), 1153–1160.
(10) Xiao, S. G.; Yang, X. M.; Edwards, E. W.; La, Y. H.; Nealey, P. F. *Nanotechnology* **2005**, *16* (7), S324–S329.
(11) *International Technology Roadmap for Semiconductors - Lithography*; International SEMATECH: Austin, TX, 2009.
(12) Yan, B.; Thubagere, A.; Premasiri, W. R.; Ziegler, L. D.; Dal Negro, L.; Reinhard, B. M. *ACS Nano* **2009**, *3* (5), 1190–1202.
(13) Maier, S. A.; Brongersma, M. L.; Kik, P. G.; Meltzer, S.; Requicha, A. A. G.; Atwater, H. A. *Adv. Mater.* **2001**, *13* (19), 1501.
(14) Coskun, U. C.; Mebrahtu, H.; Huang, P. B.; Huang, J.; Sebba, D.; Biasco, A.; Makarovski, A.; Lazarides, A.; LaBean, T. H.; Finkelstein, G. *Appl. Phys. Lett.* **2008**, *93*, 12.
(15) Ma, L. C.; Subramanian, R.; Huang, H. W.; Ray, V.; Kim, C. U.; Koh, S. J. *Nano Lett.* **2007**, *7* (2), 439–445.
(16) Edwards, E. W.; Montague, M. F.; Solak, H. H.; Hawker, C. J.; Nealey, P. F. *Adv. Mater.* **2004**, *16* (15), 1315–1319.
(17) Ruiz, R.; Kang, H.; Detcheverry, F. A.; Dobisz, E.; Kercher, D. S.; Albrecht, T. R.; de Pablo, J. J.; Nealey, P. F. *Science* **2008**, *321*, 936–939.
(18) Xiao, S.; Yang, X.; Park, S.; Weller, D.; Russell, T. P. *Adv. Mater.* **2009**, *21* (24), 2516–2519.
(19) Ji, S. X.; Liu, C. C.; Liu, G. L.; Nealey, P. F. *ACS Nano* **2010**, *4* (2), 599–609.
(20) Liu, G.; Thomas, C. S.; Craig, G. S. W.; Nealey, P. F. *Adv. Funct. Mater.* **2010**, *20* (8), 1251–1257.
(21) Han, E.; Stuen, K. O.; La, Y. H.; Nealey, P. F.; Gopalan, P. *Macromolecules* **2008**, *41* (23), 9090–9097.
(22) Cheng, J. Y.; Rettner, C. T.; Sanders, D. P.; Kim, H. C.; Hinsberg, W. D. *Adv. Mater.* **2008**, *20* (16), 3155–3158.
(23) Detcheverry, F. A.; Liu, G. L.; Nealey, P. F.; de Pablo, J. J. *Macromolecules* **2010**, *43* (7), 3446–3454.
(24) Edwards, E. W.; Stoykovich, M. P.; Muller, M.; Solak, H. H.; De Pablo, J. J.; Nealey, P. F. *J. Polym. Sci., Part B: Polym. Phys.* **2005**, *43* (23), 3444–3459.
(25) Edwards, E. W.; Muller, M.; Stoykovich, M. P.; Solak, H. H.; de Pablo, J. J.; Nealey, P. F. *Macromolecules* **2007**, *40* (1), 90–96.
(26) Ryu, D. Y.; Shin, K.; Drockenmuller, E.; Hawker, C. J.; Russell, T. P. *Science* **2005**, *308* (5719), 236–239.
(27) Solak, H. H.; David, C.; Gobrecht, J.; Golovkina, V.; Cerrina, F.; Kim, S. O.; Nealey, P. F. *Sub-50 nm Period Patterns with EUV Interference Lithography* **2003**, 56–62.
(28) Stoykovich, M. P.; Kang, H.; Daoulas, K. C.; Liu, G.; Liu, C. C.; de Pablo, J. J.; Mueller, M.; Nealey, P. F. *ACS Nano* **2007**, *1* (3), 168–175.
(29) Turkevich, J.; Stevenson, P. C.; Hillier, J. *Discuss. Faraday Soc.* **1951**, *11*, 55–75.
(30) Russell, T. P.; Coulon, G.; Deline, V. R.; Miller, D. C. *Macromolecules* **1989**, *22* (12), 4600–4606.
(31) Coulon, G.; Collin, B.; Ausserre, D.; Chatenay, D.; Russell, T. P. *J. Phys. (Paris)* **1990**, *51* (24), 2801–2811.
(32) Peters, R. D.; Yang, X. M.; Kim, T. K.; Sohn, B. H.; Nealey, P. F. *Langmuir* **2000**, *16* (10), 4625–4631.
(33) Sohn, K.; Dimitriou, M.; Genzer, J.; Fischer, D.; Hawker, C.; Kramer, E. *Langmuir* **2009**, *25* (11), 6341–6348.
(34) Ade, H.; Hitchcock, A. P. *Polymer* **2008**, *49* (3), 643–675.
(35) Detcheverry, F. A.; Pike, D. Q.; Nealey, P. F.; Muller, M.; de Pablo, J. J. *Faraday Discuss.* **2010**, *144*, 111–125.
(36) Mansky, P.; Liu, Y.; Huang, E.; Russell, T. P.; Hawker, C. *Science* **1997**, *275* (5305), 1458–1460.

(37) Tada, Y.; Akasaka, S.; Yoshida, H.; Hasegawa, H.; Dobisz, E.; Kercher, D.; Takenaka, M. *Macromolecules* **2008**, *41* (23), 9267–9276.
(38) Coulon, G.; Russell, T. P.; Deline, V. R.; Green, P. F. *Macromolecules* **1989**, *22* (6), 2581–2589.
(39) Huang, E.; Pruzinsky, S.; Russell, T. P.; Mays, J.; Hawker, C. J. *Macromolecules* **1999**, *32* (16), 5299–5303.
(40) Huang, E.; Rockford, L.; Russell, T. P.; Hawker, C. J. *Nature* **1998**, *395* (6704), 757–758.
(41) Huang, E.; Russell, T. P.; Harrison, C.; Chaikin, P. M.; Register, R. A.; Hawker, C. J.; Mays, J. *Macromolecules* **1998**, *31* (22), 7641–7650.
(42) Ade, H.; Winesett, D. A.; Smith, A. P.; Qu, S.; Ge, S.; Sokolov, J.; Rafailovich, M. *Europhys. Lett.* **1999**, *45* (4), 526–532.
(43) Liu, C. C.; Nealey, P. F.; Ting, Y. H.; Wendt, A. E. *Pattern Transfer Using Poly(styrene-block-methyl methacrylate) Copolymer Films and Reactive Ion Etching* **2007**, 1963–1968.
(44) Park, M.; Harrison, C.; Chaikin, P. M.; Register, R. A.; Adamson, D. H. *Science* **1997**, *276*, 1401–1404.
(45) Malynych, S.; Luzinov, I.; Chumanov, G. *J. Phys. Chem. B* **2002**, *106* (6), 1280–1285.
(46) Yen, A.; Smith, H. I.; Schattenburg, M. L.; Taylor, G. N. *J. Electrochem. Soc.* **1992**, *139* (2), 616–619.
(47) Liu, C.-C.; Nealey, P. F.; Raub, A. K.; Hakeem, P. J.; Brueck, S. R. J.; Han, E.; Gopalan, P. *J. Vac. Sci. Technol. B* **2010**, *28* (6), C6B30–C6B34.
(48) Cheng, J. Y.; Sanders, D. P.; Truong, H. D.; Harrer, S.; Friz, A.; Holmes, S.; Colburn, M.; Hinsberg, W. D. *ACS Nano* **2010**, *4* (8), 4815–4823.
(49) Han, E.; In, I.; Park, S. M.; La, Y. H.; Wang, Y.; Nealey, P. F.; Gopalan, P. *Adv. Mater.* **2007**, *19* (24), 4448–4452.